Journal of Alloys and Compounds 471 (2009) 291–295

Contents lists available at ScienceDirect

Journal of Alloys and Compounds

journal homepage: www.elsevier.com/locate/jallcom

Interfacial reaction between Sn–1Ag–0.5Cu(–Co) solder and Cu substrate with Au/Ni surface finish during reflow reaction

K.S. Lin [a,*], H.Y. Huang [b], C.P. Chou [a]

[a] Department of Mechanical Engineering, National Chiao Tung University, Hsinchu 300, Taiwan, ROC
[b] Department of Materials Science and Engineering, National Formosa University, Yunlin 632, Taiwan, ROC

ARTICLE INFO

Article history:
Received 27 January 2008
Received in revised form 19 March 2008
Accepted 20 March 2008
Available online 9 May 2008

Keywords:
Lead-free solder
Co addition
Interfacial reaction
Joint strength
Ball shear test

ABSTRACT

In order to clarify the effect of the addition of Co to SAC105 solder, the reaction between solder and Au/Ni surface finish has been investigated, and the joint strength was also evaluated by a ball shear test. After soldering, the interfacial reaction layer in the SAC105—Co solder contained Co, and the chemical composition of intermetallic compounds (IMCs) were identified as $(Cu,Ni,Co)_6Sn_5$ and $(Ni,Cu,Co)_3Sn_4$ by energy-dispersive X-ray spectrometer (EDX), which significantly differed from that of SAC105 solder. After multiple reflows, the formation rate of the $(Cu,Ni,Co)_6Sn_5$ IMC for the Co-added solder slow compared with that of $(Cu,Ni)_6Sn_5$ IMC for SAC105 solder. Experimental results clearly indicate that adding small amounts (0.05 wt.%) of Co to SAC105 solder strongly affected the formation of the IMC at the interface. Furthermore, ball shear test results demonstrate that the SAC105 and SAC105—Co solder joints have good joint reliability.

© 2008 Elsevier B.V. All rights reserved.

1. Introduction

Due to environmental considerations, the use of lead-free solders has become common in electronic packaging industry. Among various lead-free solders available, near-eutectic Sn—Ag—Cu alloys are considered the most promising replacement of Sn—Pb solders, and are widely used as lead-free solutions for ball-grid-array (BGA) interconnects in the microelectronic packaging industry. The industry standard employs Sn—Ag—Cu (SAC) alloys, although Sn—4 wt.% Ag—0.5 wt.% Cu (SAC405) or Sn—3 wt.% Ag—0.5 wt.% Cu (SAC305) have been already used by some companies, exhibit significantly poorer performance than eutectic Sn—Pb under high-strain rate conditions such as drop testing [1]. Thus SAC solder joints are more fragile under dynamic loads, which are frequently encountered by portable electronic devices during normal or excessive use conditions [2]. To address this challenge, drop-resistant SAC alloy development efforts have been launched by the current studies and, in recent years, considerable progress has been made in this area. Current data indicates that Ag content is controlled to modulate bulk properties of SAC alloys. Suh et al. [1] demonstrated that bulk properties of SAC alloys have significant effects on high-strain rate fracture resistance, and reducing Ag content is highly effective in increasing bulk compliance and plastic energy dissipation ability, resulting in significant performance enhancement during drop testing. Suh et al. and some other researchers [1–3] have also reported that Sn—1 wt.% Ag—0.5 wt.% Cu (SAC105) alloy and other low-Ag alloys exhibit significantly higher fracture resistance under high-strain rate conditions than SAC405 and SAC305 alloys. Nevertheless, compared with high-Ag alloys, such as SAC405 and SAC305, the SAC105 had lower elastic modulus and tensile strength due to reduced Ag content [1].

Until now, many studies have investigated the characteristics of lead-free solders, such as their microstructures, mechanical properties, and interfacial reactions. Considerable research on Sn—(3–4 wt.%) Ag—(0.5–0.75 wt.%) Cu alloys has been carried out, and the interfacial reactions between the solder and substrate have been analyzed to elucidate their interaction [4–7]. To enhance solder properties and interfacial reactions, microelements, such as Ni, Fe, Mn, Ti and Co have been added to the solder [8–17]. Anderson et al. [12] demonstrated that adding Co to SAC improved its microstructure refinement and its ability to maintain shear strength after aging. Kim et al. [14,15] and other researchers reported that adding a minor amount of Co to an SAC alloy improved tensile strength. However, studies of interfacial reactions and bonding strength of SAC105 solder joints are very limited, and the characteristics of the SAC105 alloy must be

* Corresponding author. Fax: +886 3 5720634.
E-mail address: links@ms4.url.com.tw (K.S. Lin).

0925-8388/$ – see front matter © 2008 Elsevier B.V. All rights reserved.
doi:10.1016/j.jallcom.2008.03.112

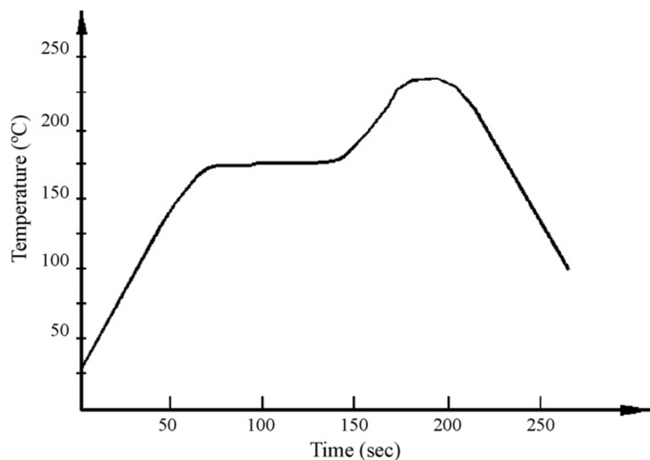

Fig. 1. Temperature profile for the reflowing process of the SAC105(—Co) solder BGA packages in this study.

studied to further improve its properties. In this study, the interfacial reaction between SAC105 and a Cu substrate with Au/Ni surface finish is investigated, and the effects of adding Co to SAC105 solder on the microstructure and mechanical properties is discussed.

2. Experimental procedures

The BGA package utilized in this study had Cu pads on a bismaleimide triazine (BT) resin substrate. The Cu pads were deposited with an Au/Ni surface finish. The thickness of the Au and Ni layers were 0.06 and 6 μm, respectively. Two solder ball types investigated in this study were Sn—1 wt.% Ag—0.5 wt.% Cu (SAC105), and Sn—1 wt.% Ag—0.5 wt.% Cu—0.05 wt.% Co (SAC105—Co) solders, each with a diameter of 0.64 mm. The solder balls were dipped in RMA flux, placed on the Au/Ni/Cu pads, and then reflowed in an IR reflow oven with nine different zones. Fig. 1 presents the reflow temperature profile, where peak temperature was set at 240 °C. This study used 1–5 solder reflow cycles. After the reflow process, specimens were cross-sectioned through a row of solder balls and polished with 0.1 μm diamond powder. The microstructures were observed via scanning electron microscopy (SEM), and their chemical compositions were analyzed using an energy-dispersive X-ray spectrometer (EDX) installed in the SEM. Bonding strengths were evaluated via ball shear tests. During these tests, ball shear rate was fixed at 0.1 mm/s. An average value from 30 measurements in each condition was adopted. After the ball shear tests, the top views of fracture surfaces were investigated thoroughly by SEM and EDX.

3. Results and discussion

Fig. 2 presents SEM micrographs of the interface between SAC105 solder and the Ni layer reflowed at 240 °C for various reflow cycles. The back-scattered electron image mode of SEM was utilized to identify distinguishable phase boundaries of interfacial layers. During the initial reflow, the topmost Au layer dissolved into the molten solder, leaving the Ni layer exposed to the molten Sn—Ag—Cu solder. The microstructure of SAC105 solder balls after reflow contained Ag_3Sn and Cu_6Sn_5 intermetallic compounds (IMCs) (Fig. 2a). Additionally, the scallop-shape ternary Sn—Cu—Ni interfacial IMC layer (IMC1) existed at the interface between SAC105 solder and the Ni layer. According to EDX analysis, the composition of the ternary IMC1 phase was 48.7 at.% Sn, 32.6 at.% Cu, and 18.7 at.% Ni. The atomic ratio of (Cu + Ni) to Sn was (32.6 + 18.7):48.7, which corresponds to the $(Cu,Ni)_6Sn_5$ phase. Jeon et al. reported a small atomic size difference between Cu and Ni, and since both have the same FCC lattice structure, the substitution of Ni into Cu_6Sn_5, without causing lattice distortion or new phase formation, was reasonable [6]. The metastable solubility of Ni into Cu_6Sn_5 may be >20 at.%. Moreover, a very thin IMC layer (IMC2) was found between the IMC1 and Ni layers. The EDX analysis iden-

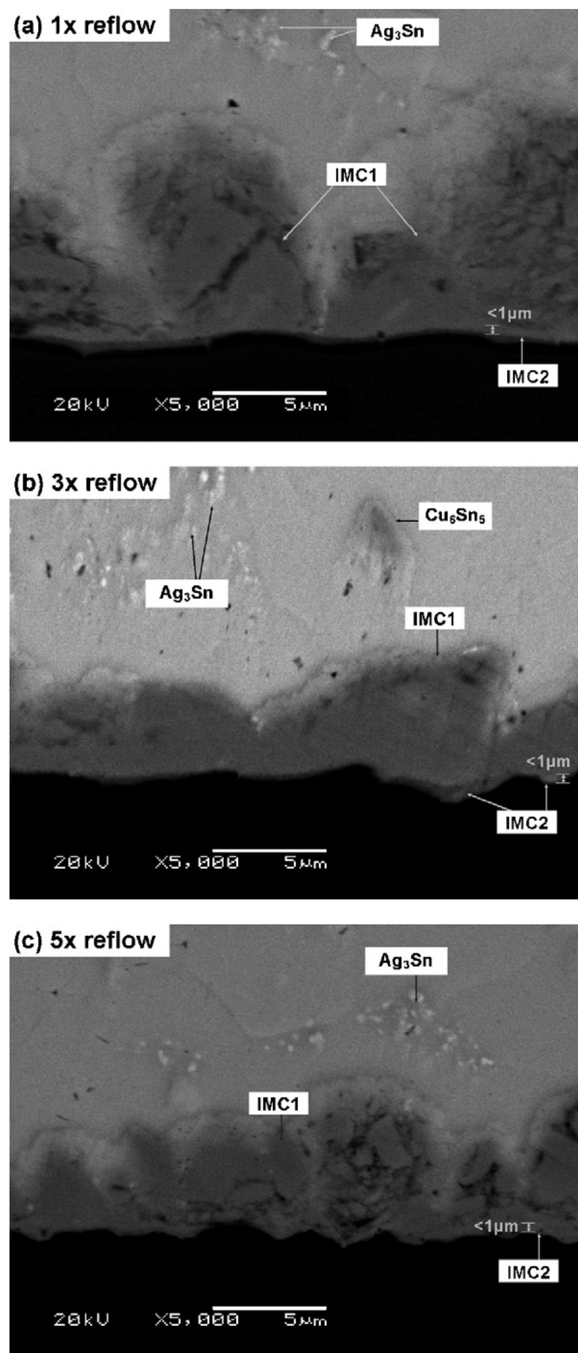

Fig. 2. SEM mircographs of SAC105 solder joint interface after various reflow cycles.

tified the composition of this very thin IMC2 layer as Ni—Cu—Sn. The atomic ratio of (Ni + Cu) to Sn was (37.5 + 10.2):52.3, which is close to 3:4. Therefore, the reaction layer adjacent to the Ni layer could be regarded as $(Ni,Cu)_3Sn_4$ IMC. Recently Suh et al. [1] reported a similar result from an investigation of the growth of IMCs formed at the interface. The formation of $(Cu,Ni)_6Sn_5$ and $(Ni,Cu)_3Sn_4$ IMCs at the interface between solder and electrolytic Ni layer were detected. Also, the very thin layer (∼20 nm) of $(Ni,Cu)_3Sn_4$ IMC was observed in both SAC105 and SAC405 systems. Jeon et al. [6] reported the formation of IMC were the same as the crystal structure of the Ni_3Sn_4 phase. Thus, the phase of this IMC must be $(Ni,Cu)_3Sn_4$ that consists of the Ni_3Sn_4-crystal structure with 4–7 at.% Cu atoms in the Ni sublattice. Similar analytical results were existed for all other

Sn—Ag—Cu solders, such as Sn—4Ag—0.5Cu, and Sn—3.5Ag—0.7Cu solders joints on the Ni layer [4–7]. Fig. 2b and c present SEM micrographs of the SAC105 samples after multiple reflows (three and five times). With an increased number of reflows, the composition of the interfacial reaction product between the solder and Ni layer was $(Cu,Ni)_6Sn_5$ and $(Ni,Cu)_3Sn_4$ phases (IMC1 and IMC2), and the scallop-shaped IMC1 layer becomes more continuous. However, the thickness of the IMC1 and IMC2 layers did not change significantly with the reflow cycle, as will be discussed.

Fig. 3 presents SEM micrographs of the interface between SAC105—Co solder and Ni layer reflowed at 240 °C for various reflow cycles. Fig. 3a shows the interface between SAC105—Co solder and the Ni layer after one reflow. A discontinuous IMC (IMC3) and a relatively thin and continuous IMC layer (IMC4) were present at the interface. Additionally, the IMC4 layer was adjacent to the Ni layer. On the other hand, IMC3 was formed at the interface between the IMC4 layer and the solder. In this study, the composition of the discontinuous IMC3 phase by EDX analysis was 49.7 at.% Sn, 32.3 at.% Cu, 15.7 at.% Ni, and 2.3 at.% Co. The IMC3 phase was likely $(Cu,Ni,Co)_6Sn_5$, reflecting a compositional ratio (6:5) between Cu + Ni + Co and Sn. Furthermore, the elemental composition of the continuous IMC4 layer was 52.4 at.% Sn, 9.9 at.% Cu, 35.3 at.% Ni, and 2.4 at.% Co; the IMC4 corresponds to the $(Ni,Cu,Co)_3Sn_4$ phase. The $(Cu,Ni,Co)_6Sn_5$ and $(Ni,Cu,Co)_3Sn_4$ IMC phases were formed by substituting Co for Cu atom in compounds with Sn. Similar experimental results were found for all other solders with Co added [13–17]. Additionally, Gao et al. [16] reported that the concentration of Co in the interfacial IMC region may be attributed to enhance the driving force of IMC formation and reduce the interfacial energy between the IMC and solder matrix during soldering. Fig. 3b and c show SEM micrographs of SAC105—Co samples after multiple reflows (three and five times). The quantities and size of the discontinuous IMC3 did not change significantly after three reflows, and became continuous after five reflows. However, the thickness of the underneath IMC4 layer increased slightly as reflow cycles increased.

Table 1 presents quantitative results of EDX analysis for interfacial IMCs. A difference existed in composition of IMCs between SAC105 and SAC105—Co alloys. For the SAC105 solder, the interfacial IMCs were estimated as $(Cu,Ni)_6Sn_5$ and $(Ni,Cu)_3Sn_4$ phases. For the SAC105—Co, the IMC layer contained Co and was estimated as $(Cu,Ni,Co)_6Sn_5$ and $(Ni,Cu,Co)_3Sn_4$ phases. However, these IMCs, $(Cu,Ni)_6Sn_5$ or $(Cu,Ni,Co)_6Sn_5$ and $(Ni,Cu)_3Sn_4$ or $(Ni,Cu,Co)_3Sn_4$, are based on the Cu_6Sn_5 and Ni_3Sn_4 crystal structures, respectively. Fig. 4 presents schematically the morphology of the IMC at the interface. For the SAC105 solder, the morphology of the $(Cu,Ni)_6Sn_5$ IMC layer is scallop-shaped and continuous, and a very thin layer of $(Ni,Cu)_3Sn_4$ was existed at the interface between the Ni layer and $(Cu,Ni)_6Sn_5$ IMC layer after multiple reflows (Fig. 4a). For the SAC105—Co solder, both $(Cu,Ni,Co)_6Sn_5$ and $(Ni,Cu,Co)_3Sn_4$ were present at the interface after one reflow (Fig. 4b). Similar to its counterpart with three reflows, the $(Cu,Ni,Co)_6Sn_5$ phase was discontinuous, whereas that of $(Ni,Cu,Co)_3Sn_4$ was continuous. However, after five reflows, discontinuous $(Cu,Ni,Co)_6Sn_5$ IMC

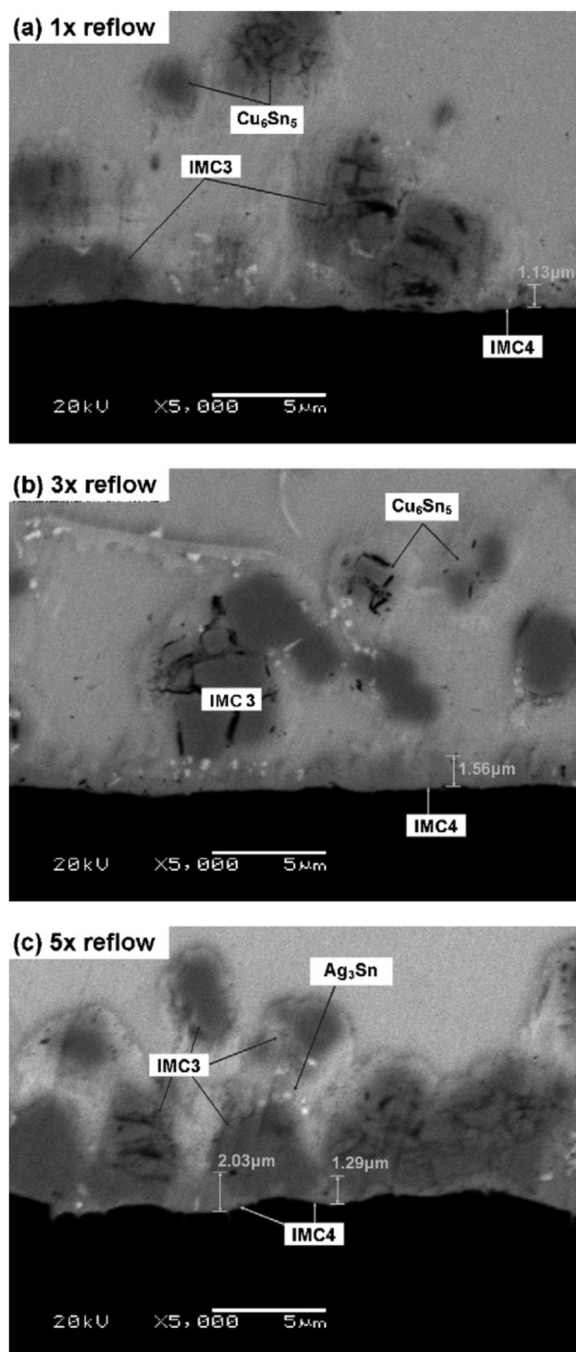

Fig. 3. SEM mircographs of SAC105—Co solder joint interface after various reflow cycles.

Table 1
EDX composition analysis results of IMCs formed at the interface

Solder	Composition (at.%)				IMC phase	
	Sn	Cu	Ni	Co		
SAC105	47.4–48.8	31.1–32.8	18.6–21.6	–	IMC1	$(Cu,Ni)_6Sn_5$
	52.1–54.8	9.8–11.5	34.2–36.4	–	IMC2	$(Ni,Cu)_3Sn_4$
SAC105—Co	48.9–49.9	32.2–33.5	13.7–16.4	1.3–2.8	IMC3	$(Cu,Ni,Co)_6Sn_5$
	52.7–54.3	9.3–10.6	33.6–35.3	1.5–2.7	IMC4	$(Ni,Cu,Co)_3Sn_4$

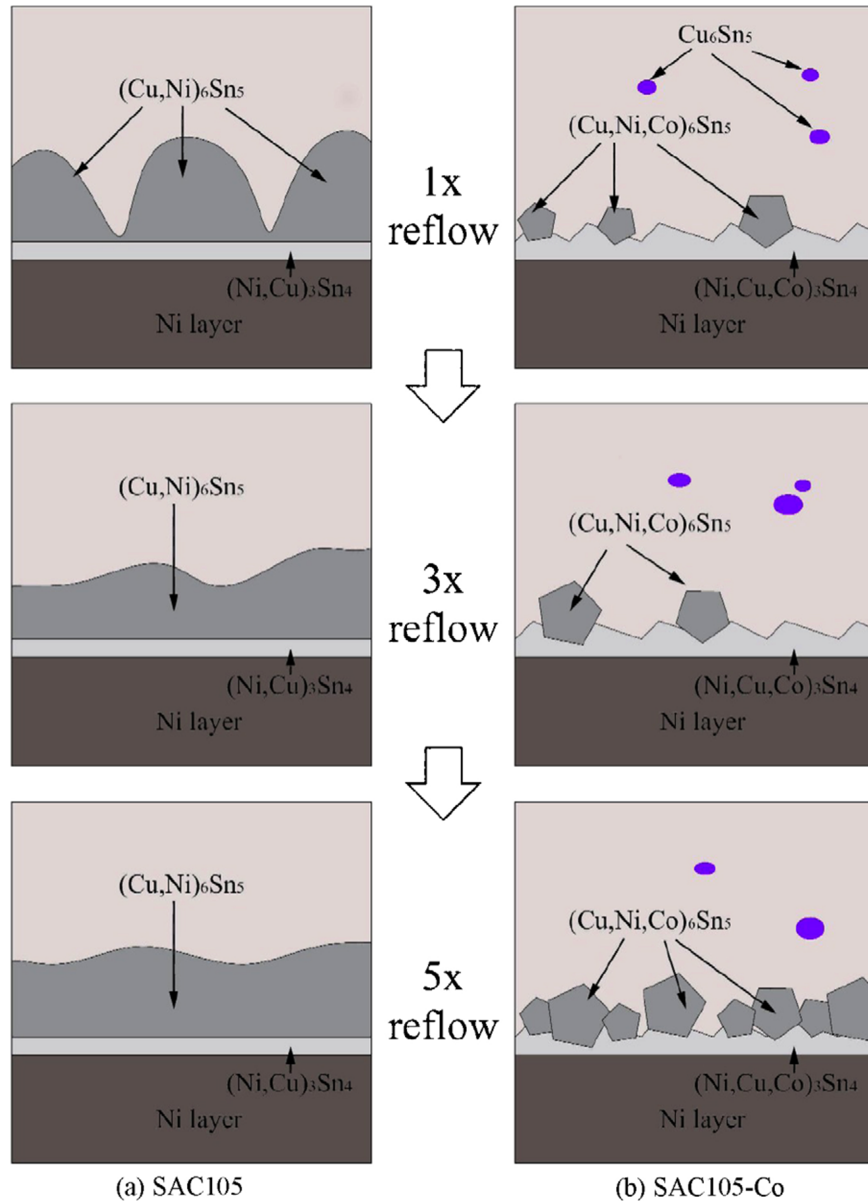

Fig. 4. Schematic diagrams of IMC changes during various reflow cycles.

changed gradually to continuous. There is one possible origin for the interfacial IMCs formation. The layered structure of IMCs may be a clue to understanding the diffusion mechanism. During soldering, the most Cu was pinned on the Sn in the form of Cu_6Sn_5 particles in the solder ball, and the remaining partial Cu was on the solder/Ni interface forming $(Ni,Cu)_3Sn_4$ or $(Ni,Cu,Co)_3Sn_4$ and $(Cu,Ni)_6Sn_5$ or $(Cu,Ni,Co)_6Sn_5$ compounds. However, the exact reason for the formation of this discontinuous $(Cu,Ni,Co)_6Sn_5$ IMC remains unclear, and it is probably since the addition of small amounts of Co in the solder may cause suppressing Cu diffusion from the solder to the interface. In this study, the average Cu contents in the SAC105(—Co) solders were fixed 0.5 wt.%. Two IMCs of $(Cu,Ni)_6Sn_5$ and $(Cu,Ni,Co)_6Sn_5$ were formed due to the Cu atoms diffusion from bulk solder to interface. However, the morphology of $(Cu,Ni)_6Sn_5$ IMC layer in the SAC105 solder joint was continuous after one reflow process, and a continuous $(Cu,Ni,Co)_6Sn_5$ layer was formed in the Co-added solder joint after five reflows. The decreasing formation rate of $(Cu,Ni,Co)_6Sn_5$ IMC during reflow process might be attributed to the diffusion of Cu atoms from solder to

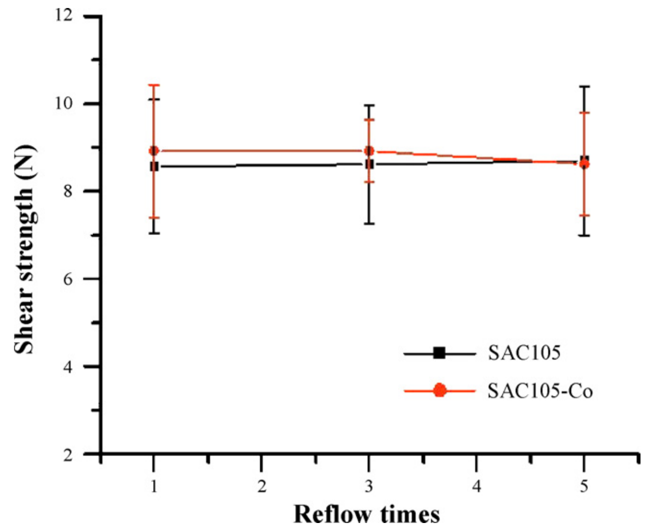

Fig. 5. Variations of the ball shear strength with reflow cycle.

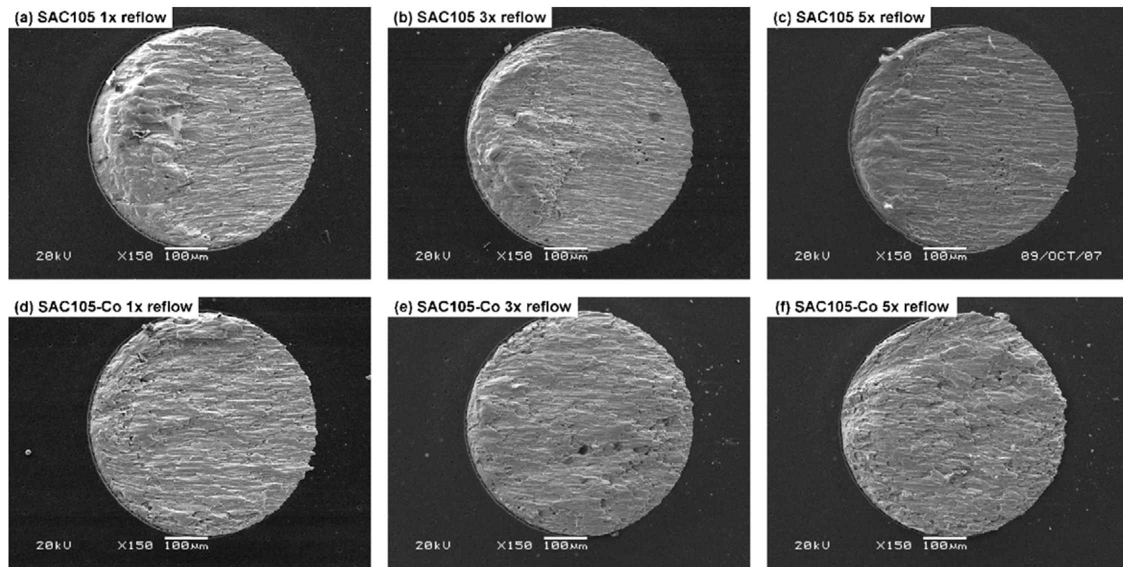

Fig. 6. Fracture surfaces of SAC105(—Co) solder joints after various reflow cycles.

interface becomes difficult. Further studies are needed to elucidate this phenomenon.

Ball shear tests were performed to evaluate the effect of interfacial reactions on solder joint reliability as a function of reflow cycles. Fig. 5 shows the ball shear strength values for SAC105(—Co) solder/Ni BGA joints with various reflow cycles. Little difference was observed in the strength between SAC105 and SAC105—Co samples. Additionally, shear strength did not change much as a function of reflow cycles. Mean shear strength was 8–9 N in this study, indicating that shear strength of the SAC105 and SAC105—Co joints was not sensitive to the number of reflow cycles such as five times at 240 °C. After the ball shear tests, fractured surfaces were examined by SEM. Fig. 6 presents top views of the fractured surfaces for SAC105(—Co) solder joints reflowed for various reflow cycles. The fracture of all specimens after ball shear tests indicates ductility across the solder balls (Fig. 6). Additionally, the interfacial IMCs, such as $(Cu,Ni,Co)_6Sn_5$ and $(Ni,Cu,Co)_3Sn_4$ were not observed on the fractured surfaces. Generally, a fracture occurs during the ball shear test at the interface in the weakest solder region. In this study, ball shear test results indicated that shear strength of the SAC105(—Co) solder joint could not be significantly related to the type of IMCs formed at the interface. Consequently, interfacial reaction and shear test results in this study show that the SAC105 and SAC105—Co solder joints have a desirable joint reliability.

4. Conclusions

The formation of IMCs at the interface between SAC105(—Co) solder and a Ni layer were investigated. Joint strength was also evaluated using ball shear tests to reveal the effects of adding Co to SAC105 solder. The primary experimental results obtained in this study are summarized as follows:

(1) After reflowing, the reaction between SAC105—Co solder and the Ni layer resulted in formation of two IMCs, such as $(Cu,Ni,Co)_6Sn_5$ and $(Ni,Cu,Co)_3Sn_4$, at the interface. The morphology of the $(Cu,Ni,Co)_6Sn_5$ IMC layer was discontinuous, and $(Ni,Cu,Co)_3Sn_4$ IMC layer was thin and continuous.
(2) For SAC105 solder, the morphology of the $(Cu,Ni)_6Sn_5$ IMC layer was continuous after one reflow. For the SAC105—Co solder, discontinuous $(Cu,Ni,Co)_6Sn_5$ IMC changed gradually to continuous after five reflows. The decreased formation rate of $(Cu,Ni,Co)_6Sn_5$ IMC during reflowing was attributed to the addition of small amounts of Co in the solder suppressing Cu diffusion from the solder to the interface.
(3) In the ball shear tests, adding Co to SAC105 solder did not influence the shear strength of the solder joints, and the shear strength value did not change significantly as a function of number of reflow cycles. Moreover, for both SAC105 and SAC105—Co solder joints, fractures occurred in the solder ball. Shear test results demonstrate that SAC105 and SAC105—Co solder joints have good joint reliability.

References

[1] D. Suh, D.W. Kim, P. Liu, H. Kim, J.A. Weninger, C.M. Kumar, A. Prasad, B.W. Grimsley, H.B. Tejada, Mater. Sci. Eng. A. 460/461 (2007) 595.
[2] Y.S. Lai, P.F. Yang, C.L. Yeh, Microelectron. Reliab. 46 (2006) 645.
[3] S.T. Jenq, H.S. Sheu, C.L. Yeh, Y.S. Lai, J.D. Wu, Int. J. Impact Eng. 34 (2007) 1655.
[4] P. Sun, C. Andersson, X. Wei, Z. Cheng, D. Shangguan, J. Liu, J. Alloys Comp. 425 (2006) 191.
[5] J.W. Yoon, S.W. Kim, S.B. Jung, J. Alloys Comp. 392 (2005) 247.
[6] Y.D. Jeon, S. Nieland, A. Ostmann, H. Reichl, K.W. Paik, J. Electron. Mater. 32 (2003) 548.
[7] L.Y. Hsiao, S.T. Kao, J.G. Duh, J. Electron. Mater. 35 (2006) 81.
[8] T.H. Chuang, S.F. Yen, M.D. Cheng, J. Electron. Mater. 35 (2006) 302.
[9] T.H. Chuang, S.F. Yen, H.M. Wu, J. Electron. Mater. 35 (2006) 310.
[10] H. Nishikawa, J.Y. Piao, T. Takemoto, J. Electron. Mater. 35 (2006) 1127.
[11] F. Gao, T. Takemoto, H. Nishikawa, J. Electron. Mater. 35 (2006) 2081.
[12] I.E. Anderson, B.A. Cook, J. Harringa, R.L. Terpstra, J. Electron. Mater. 31 (2002) 1166.
[13] J.C. Foley, A. Gickler, F.H. Leprevost, D. Brown, J. Electron. Mater. 29 (2000) 1258.
[14] K.S. Kim, S.H. Huh, K. Suganuma, Microelectron. Reliab. 43 (2003) 259.
[15] J.M. Song, C.F. Huang, H.Y. Chuang, J. Electron. Mater. 35 (2006) 2154.
[16] F. Gao, T. Takemoto, H. Nishikawa, A. Komatsu, J. Electron. Mater. 35 (2006) 905.
[17] H. Nishikawa, A. Komatsu, T. Takemoto, J. Electron. Mater. 36 (2007) 1137.